

Original Article

Identification of a dominant murine T-cell epitope in recombinant protein P29 from *Echinococcus granulosus*

Yongxue Lv^{1,2,†}, Yazhou Zhu^{1,†}, Liangliang Chang¹, Jihui Yang^{1,2}, Yinqi Zhao¹, Jiaqing Zhao^{1,2}, Yana Wang¹, Mingxing Zhu¹, Changyou Wu³, and Wei Zhao^{1,2,*}

¹School of Basic Medicine, Ningxia Medical University, Yinchuan 750004, China, ²Department of Pathogen Biology and Medical Immunology, Ningxia Medical University, Yinchuan 750004, China, and ³Institute of Immunology, Zhongshan School of Medicine, Sun Yat-sen University Guangzhou 5102275, China

[†]These authors contributed equally to this work.

*Correspondence address. Tel: +86-13895112892; E-mail: zw-6915@163.com

Received 2 October 2021 Accepted 11 November 2021

Abstract

Echinococcus granulosus causes echinococcosis, an important zoonotic disease worldwide and a major public health issue. Vaccination is an economical and practical approach for controlling *E. granulosus*. We have previously revealed that a recombinant protein P29 (rEg.P29) is a good vaccine candidate against *E. granulosus*. However, T cell immunogenic epitopes have not been identified. In the present study, we use rEg.P29-immunized mice as models to screen immunogenic epitopes for the construction of a novel multi-epitope vaccine. We search for immunodominant epitopes from an overlapping peptide library to screen the peptides of rEg.P29. Our results confirm that rEg.P29 immunization in mice elicits the activation of T cells and induces cellular immune responses. Further analyses show that a T cell epitope within amino acids 86–100 of rEg.P29 elicits significant antigen-specific IFN- γ production in CD4⁺ and CD8⁺ T cells and promotes specific T-cell activation and proliferation. Collectively, these results provide a reference for the construction of a novel vaccine against broad *E. granulosus* genotypes based on epitopes of rEg.P29.

Key words *Echinococcus granulosus*, rEg.P29, T-cell epitope

Introduction

Echinococcus granulosus is a cause of potentially lethal zoonotic infections characterized by space-occupying lesions worldwide, especially in areas of animal husbandry. In endemic areas, the annual incidence of echinococcosis is 1/100,000 to 200/100,000, and the mortality of cystic echinococcosis (CE) is 2%–4% [1]. The World Health Organization estimated that 91% of new cases of hepatic encysted liver disease worldwide each year occur in China [2]. It is one of 17 diseases identified, as it is easily overlooked by the WHO [3].

According to established guidelines [4], treatment options for human echinococcosis include: (i) radical hepatectomy as the first choice, (ii) long-term chemotherapy in cases where surgery is not possible or only partial resection is possible, and (iii) anti-infective drug treatment. However, the risk of recurrence represents a major issue [5–7]. Furthermore, population screening has shown that CE liver cysts in humans grow very slowly. Human echinococcosis

lacks symptoms in the early stages of development and is often diagnosed at a late stage. Therefore, vaccination is expected to be an effective way against *E. granulosus* [8].

The P29 protein was first described by Excler *et al.* [9] as a novel 29 kDa antigen from *E. granulosus* protoscoleces. As a diagnostic antigen, it has a high sensitivity and specificity (*i.e.*, 88% and 89.9%, respectively) [10]. We have previously found that rEg.P29 shows 94.5% protective efficacy in a sheep model with secondary infection and could induce strong cellular and humoral immune responses against *E. granulosus* [11]. In view of these data for rEg.P29, a multi-epitope vaccine containing proper antigenic peptides may serve as an efficient vaccine against *E. granulosus* infection.

Reverse vaccinology targeting the development of multi-epitope vaccines is a promising strategy [12]. Compared with conventional vaccines, epitope vaccines are relatively safe, stable, and can selectively initiate multiple immune responses. Epitope vaccines have been studied extensively in the context of the prevention and

treatment of tumors, tuberculosis, dust mite, parasites, and other diseases [13–16], representing a new direction for vaccine development. The T cell-mediated cellular immune response [17,18] and B cell-mediated humoral immune response [19,20] play important roles in protection against *E. granulosus*.

In this study, we searched for immunodominant epitopes based on experimental evaluations of candidate epitopes identified from overlapping peptide libraries, and provided a reference for the development of rEg.P29 epitope vaccines.

Materials and Methods

Antigen preparation

The complete amino acid sequence of rEg.P29 was obtained from the NCBI database (AAD53328.1). The recombinant protein expression and purification were performed following the previously published methods [21]. In brief, expression was induced at 37°C for 10 h in the presence of 50 µg/mL isopropyl-β-d-thiogalactoside (IPTG; Invitrogen, Waltham, USA). Then, the rEg.P29 protein was purified using the His Purification kit (Merck, Kenilworth, USA) according to the manufacturer's instructions. The purified rEg.P29 was identified by SDS-PAGE, and the protein concentration was detected using the BCA kit (KeyGEN BioTECH, Nanjing, China). The 45 overlapping peptides of rEg.P29 (Table 1) and CpG ODN 1826 (TCCATGACGTTCTGACGTT) were synthesized by Sangon (Shanghai, China). The purity of the synthesized peptide was ≥98%, as determined by high-performance liquid chromatography, and the content, sterility, and the absence of endotoxin were confirmed. The dry powder was dissolved to a concentration of 1 mg/mL and stored at -80°C.

Animals and immunizations

Six to eight-week-old female specific pathogen-free C57BL/6 mice (SCXK2016-0006) were provided by the Animal Center of Ningxia Medical University. The study was approved by the Experimental Animal Ethics Committee of Ningxia Medical University and experiments were carried out in strict accordance with national and institutional guidelines. Mice were randomly assigned into 3 groups, i.e., control group (injected with PBS only), rEg.P29 + FCA group (injected with 20 µg rEg.P29 emulsified with FCA), and rEg.P29 + CpG group (injected with 20 µg rEg.P29 and 20 µg CpG ODN 1826). For the subcutaneous immunization, the emulsified mixture was suspended in phosphate-buffered saline (PBS) and injected into the lower quadrant of the abdomen (100 µL/mouse). One week later, the purified proteins were mixed with Freund's incomplete adjuvant or CpG ODN 1826 as protein vaccines to boost immunity. We performed two boost, as shown in Figure 1.

Sample collection and cell culture

At indicated time after immunization, mice were anesthetized with chloral hydrate, serum samples and the splenic tissues were collected from each mouse. Spleen cells were isolated immediately by pushing the spleen through a 70-µm strainer in Hank's balanced salt solution, followed by Ficoll-Hypaque (Tianjin HaoYang Biological Manufacture, Tianjin, China) density gradient centrifugation at 450 g for 20 min. Mononuclear cells were collected, washed twice with Hank's balanced salt solution, and re-suspended at a final concentration of 2×10^6 cells/mL in complete RPMI 1640 medium (HyClone, Logan, USA) supplemented with 10% heated-inactivated fetal calf serum (FCS; GeminiBio, West Sacramento,

Table 1. Amino acid sequences of overlapping peptides

No.	Name	Sequence	Length
ID1	rEg.P29 ₁₋₁₅	MSGFDVTKTFNRFTQ	15
ID2	rEg.P29 ₆₋₂₀	VTKTFNRFTQRAGEL	15
ID3	rEg.P29 ₁₁₋₂₅	NRFTQRAGELVKNKE	15
ID4	rEg.P29 ₁₆₋₃₀	RAGELVKNNEKTSYP	15
ID5	rEg.P29 ₂₁₋₃₅	VKNNEKTSYPTRTSD	15
ID6	rEg.P29 ₂₆₋₄₀	KTSYPTRTSDLIHEI	15
ID7	rEg.P29 ₃₁₋₄₅	TRTSDLIHEIDQMKA	15
ID8	rEg.P29 ₃₆₋₅₀	LIHEIDQMKAWISKI	15
ID9	rEg.P29 ₄₁₋₅₅	DQMKAWISKIITATE	15
ID10	rEg.P29 ₄₆₋₆₀	WISKIITATEEFVDI	15
ID11	rEg.P29 ₅₁₋₆₅	ITATEEFVDINIASK	15
ID12	rEg.P29 ₅₆₋₇₀	EFVDINIASKVADAF	15
ID13	rEg.P29 ₆₁₋₇₅	NIASKVADAFQKNKE	15
ID14	rEg.P29 ₆₆₋₈₀	VADAFQKNKEKITTT	15
ID15	rEg.P29 ₇₁₋₈₅	QKNKEKITTTDKLGT	15
ID16	rEg.P29 ₇₆₋₉₀	KITTTDKLGTALQV	15
ID17	rEg.P29 ₈₁₋₉₅	DKLGTALQVASQSE	15
ID18	rEg.P29 ₈₆₋₁₀₀	ALEQVASQSEKAAPQ	15
ID19	rEg.P29 ₉₁₋₁₀₅	ASQSEKAAPQLSKML	15
ID20	rEg.P29 ₉₆₋₁₁₀	KAAPQLSKMLTEASD	15
ID21	rEg.P29 ₁₀₁₋₁₁₅	LSKMLTEASDVHQRM	15
ID22	rEg.P29 ₁₀₆₋₁₂₀	TEASDVHQRMATARK	15
ID23	rEg.P29 ₁₁₁₋₁₂₅	VHQRMATARKNFNSE	15
ID24	rEg.P29 ₁₁₆₋₁₃₀	ATARKNFNSEVNTTF	15
ID25	rEg.P29 ₁₂₁₋₁₃₅	NFNSEVNTTFIEDLK	15
ID26	rEg.P29 ₁₂₆₋₁₄₀	VNTTFIEDLKNFLNT	15
ID27	rEg.P29 ₁₃₁₋₁₄₅	IEDLKNFLNTTLLSEA	15
ID28	rEg.P29 ₁₃₆₋₁₅₀	NFLNTTLLSEAQKAKT	15
ID29	rEg.P29 ₁₄₁₋₁₅₅	TLSEAQKAKTKLEEV	15
ID30	rEg.P29 ₁₄₆₋₁₆₀	QKAKTKLEEVRLDLD	15
ID31	rEg.P29 ₁₅₁₋₁₆₅	KLEEVRLDLDSDKTK	15
ID32	rEg.P29 ₁₅₆₋₁₇₀	RLDLDSDKTKLKNKAK	15
ID33	rEg.P29 ₁₆₁₋₁₇₅	SDKTKLKNKAKTAEQK	15
ID34	rEg.P29 ₁₆₆₋₁₈₀	LKNKAKTAEQKAKWEA	15
ID35	rEg.P29 ₁₇₁₋₁₈₅	TAEQKAKWEAEVRKD	15
ID36	rEg.P29 ₁₇₆₋₁₉₀	AKWEAEVRKDESDFD	15
ID37	rEg.P29 ₁₈₁₋₁₉₅	EVRKDESDFDRVHQE	15
ID38	rEg.P29 ₁₈₆₋₂₀₀	ESDFDRVHQESLTIF	15
ID39	rEg.P29 ₁₉₁₋₂₀₅	RVHQESLTIFEKTCCK	15
ID40	rEg.P29 ₁₉₆₋₂₁₀	SLTIFEKTCCKEFDGL	15
ID41	rEg.P29 ₂₀₁₋₂₁₅	EKTCCKEFDGLSVQLL	15
ID42	rEg.P29 ₂₀₆₋₂₂₁	EFDGLSVQLLLDLIRA	15
ID43	rEg.P29 ₂₁₁₋₂₂₅	SVQLLLDLIRAEKNYY	15
ID44	rEg.P29 ₂₁₆₋₂₃₁	DLIRAEKNYYEACAK	15
ID45	rEg.P29 ₂₂₁₋₂₃₅	EKNYYEACAKECSMM	15

USA), 100 µg/mL streptomycin, 100 U/mL penicillin, 2 mM L-glutamine, and 50 µM 2-mercaptoethanol (Gibco, Grand Island, USA).

Prime&Boost Groups

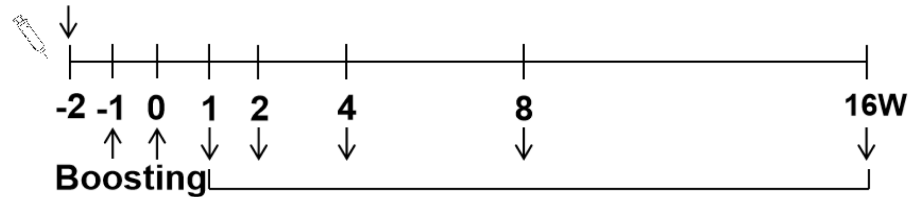
S.C.:

1.PBS

2.rEg.P29+FCA

3.rEg.P29+CpG

Priming



Sample testing

Figure 1. Scheme of immunization and sampling C57BL/6 mice ($n=5-7$ /group) were subcutaneously immunized following the prime-boost protocol. We performed two boosts (-1 and 0). Spleen sample and serum sample were collected and tested at indicated time points.

ELISA and ELISpot

Mononuclear cells were suspended in complete RPMI 1640 medium at density of 2×10^6 cells/mL. A total of 200 μ L cell suspension was seeded into each well of a round-bottom 96-well plate, and stimulated with or without rEg.P29 or peptides (15 μ g/mL) in the presence of anti-CD28 (1 μ g/mL) at 37°C with 5% CO₂ for 3 days. Cytokines (IFN- γ , TNF- α , IL-2, IL-4, and IL-10) in the supernatants were detected using BD OptEIA Mouse ELISA Sets (BD Biosciences, San Jose, USA) according to the manufacturer's instructions. Reactions were stopped with 1 M H₂SO₄, and the optical density of each well was measured at 450 nm using a microplate reader (Thermo Fisher, Waltham, USA). Concentrations were calculated using standard serial dilutions of cytokines.

For the ELISpot assay of cytokine-producing cells, mononuclear cells were suspended in complete RPMI 1640 medium at density of 1×10^6 cells/mL. Then, 100 μ L of cell suspension was seeded into each well of pre-coated BD ELISpot plates (BD Biosciences) and stimulated with or without rEg.P29 or peptides (15 μ g/mL) in the presence of anti-CD28 (1 μ g/mL) at 37°C with 5% CO₂ for 24 h. After being washed with RPMI 1640 medium, the plates were incubated with biotinylated detecting antibodies (BD Biosciences), followed by incubation with streptavidin-HRP (BD Biosciences). AEC substrate (BD Biosciences) was added to the wells for spot development, and the reaction was stopped by washing the wells with deionized water. The plate was air-dried at room temperature, and IFN- γ and IL-4-producing cells were enumerated using AID Classic ELR08 (Aid Autoimmun Diagnostika GmbH, Straßberg, Germany) according to the manufacturer's instructions. The results are shown as the mean values from triplicate wells.

Flow cytometric analysis

To measure the level of intracellular cytokines, cells were suspended in culture medium at a concentration of 1×10^6 cells/mL and cultured with or without rEg.P29 or peptides at 15 μ g/mL in the presence of anti-CD28 (1 μ g/mL) at 37°C with 5% CO₂ for 20 h. Brefeldin A (Sigma-Aldrich, St Louis, USA) was added to the culture during the final 6 h at concentration of 10 μ g/mL. The cells were washed twice with PBS containing 0.1% bovine serum albumin and 0.05% sodium aside (Buffer 1), followed by staining with fluorochrome-conjugated monoclonal antibodies (mAbs) for phenotyping for 30 min at 4°C in the dark. Then, the cells were washed with Buffer 1, fixed with 4% paraformaldehyde and permeabilized with Buffer 2 (Buffer 1 with 0.1% saponin) overnight at 4°C. After staining for the detection of intracellular cytokines with fluor-

ochrome-conjugated monoclonal antibodies for 30 min at 4°C in the dark, cells were washed with Buffer 1 and evaluated using the FACSCelesta (BD Biosciences) for data collection. Data were analyzed using FlowJo 10 (TreeStar, San Carlos, USA). For phenotyping, cells were washed with Buffer 1, and then stained with phenotyping mAbs for 30 min at 4°C in the dark. The following fluorochrome-antibodies were purchased from BD Biosciences and used for flow cytometric analysis: Phycoerythrin-Texas Red (PE-CF594) conjugated-anti-CD3 antibody, Allophycocyanin-Cyanin 7 (APC-Cy7) conjugated-anti-CD4 antibody, Pacific Blue conjugated-anti-CD8 antibody, Fluorescein isothiocyanate (FITC) conjugated-anti-IFN- γ antibody, Phycoerythrin (PE) conjugated-anti-CD25 antibody, and Alexa Fluor conjugated-anti-CD69 antibody. Fixable Viability Dye eFluor™506 was obtained from Invitrogen.

Cell proliferation assay

To evaluate proliferation, cells were washed twice with pre-warmed PBS. Carboxyfluorescein diacetate succinimidylester (CFSE; Invitrogen) at a concentration of 2.5 μ M was added and incubated for 15 min at 37°C in the dark. The reaction was terminated with precooled PBS (containing 10% FBS), incubated at 4°C for 5 min, and washed twice with precooled PBS. CFSE-labeled cells were then cultured with or without rEg.P29 or peptide at 15 μ g/mL for the indicated time at 37°C with 5% CO₂. Cell samples were collected and stained with fluorochrome-conjugated monoclonal antibodies for phenotyping at 4°C in the dark. Then, samples were assayed using the FACSCelesta. Data were analyzed using FlowJo.

Multiple sequence alignment

To determine whether the core epitope was conserved among P29 proteins, the P29 protein amino acid sequences of *E. granulosus* reported by Boubaker *et al.* [22] were analyzed. Homology between rEg.P29₈₆₋₁₀₀ in the P29 protein and different *E. granulosus s.l.* isolates were compared using BLAST (<https://blast.ncbi.nlm.nih.gov/Blast.cgi>) and Jalview (Version 2.11.1.5).

Localization of the core epitope on rEg.P29

SWISS-MODEL (<https://swissmodel.expasy.org/interactive>) was used to predict the three-dimensional structure of rEg.P29. Two threading templates were selected by this program for construction (2d4c.1.A and 6up6.1). Core epitope was mapped against the three-dimensional structure.

Statistical analysis

All statistical tests were performed using GraphPad Prism 8.0 (GraphPad Software Inc., San Diego, USA) and SPSS 22.0. The unpaired Student's *t*-test was used for comparisons between two groups and one-way or two-way ANOVA was used for comparisons among more than two groups. The LSD test or SNK test was used for data with normal distribution and homogeneous variance. Dunnett's T3 test or independent sample *t*-test was used for data that conformed to normal distribution but had uneven variance. Data are presented as the mean or the mean \pm SD. $P < 0.05$ was considered statistically significant.

Results

rEg.P29 induces a cellular immune response

rEg.P29 was first expressed in *Escherichia coli* and purified using a His-Affinity Agarose column, as shown in [Supplementary Figure S1](#). To explore the preventive effect of rEg.P29 against *E. granulosus*, we immunized mice subcutaneously with rEg.P29 plus Freund's adjuvant (rEg.P29 + FCA) and rEg.P29 plus CpG (rEg.P29 + CpG) respectively, as summarized in [Figure 1](#). Control mice were injected with PBS only. Lymphocytes were prepared from the spleen of immunized mice from week 1 to week 16.

After *in vitro* rEg.P29 stimulation, the production of cytokines was evaluated in lymphocytes isolated from the spleen of immunized mice. Cells from mice immunized with rEg.P29 + FCA and rEg.P29 + CpG produced higher levels of cytokines than those of cells from controls ([Figure 2A](#)). The IFN- γ , IL-2, and TNF- α levels peaked at week 2, and then gradually decreased to week 16, while the levels of IL-4 and IL-10 were not detectable during this time period. These results indicated that immunization with rEg.P29 + FCA and rEg.P29 + CpG established a cellular immune response in our mouse model.

Flow cytometry was used to analyze the subtypes of cells that respond to rEg.P29. Lineage differentiation by flow cytometry indicated that most cytokine-producing cells were CD3⁺T cells ([Figure 2B,C](#)). Cells from rEg.P29 + FCA and rEg.P29 + CpG-immunized mice produced the highest levels of IFN- γ ([Figure 2D,E](#)) after induction with rEg.P29, with higher frequencies of IFN- γ -producing cells than the cells from control mice (all $P < 0.0001$). These results are consistent with those of the quantitative ELISA. The cytokine-producing T cells included both CD4⁺ and CD8⁺T cells, and there was no significant difference in the frequencies of these cell types. These data suggested that rEg.P29 could stimulate the induction of IFN- γ production by CD4⁺ and CD8⁺ T cells.

rEg.P29 contains an immunodominant epitope of T cells

Overlapping peptides were used to screen epitopes recognized by rEg.P29-specific T cells. These peptides were 15-mers, overlapping by 10 amino acids and spanning the entire region of the rEg.P29 sequence ([Figure 3A](#)). By quantitative ELISA, we found that ID16-18 induced mononuclear cells isolated from mice immunized with rEg.P29 + FCA and rEg.P29 + CpG to produce IFN- γ and IL-2 ([Figure 3B,C](#)). Next, ID15, ID16, ID17, ID18, and ID19 were used to stimulate mononuclear cells isolated from PBS-, rEg.P29 + FCA-, and rEg.P29 + CpG-immunized mice ([Figure 3D,E](#)). We found that ID18 and ID19 stimulated significantly higher levels of IL-2 and IFN- γ than those in the control group.

Given these results, we then synthesized ID18 (rEg.P29₈₆₋₁₀₀), ID19 (rEg.P29₉₁₋₁₀₅), and their overlaps (rEg.P29₈₆₋₁₀₅ and

rEg.P29₉₁₋₁₀₀) ([Table 2](#)). The levels of IL-2 and IFN- γ production elicited by rEg.P29₈₆₋₁₀₀ and rEg.P29₈₆₋₁₀₅ were lower than those elicited by rEg.P29 and were significantly higher than those elicited by the medium control ([Figure 3F,G](#)).

Using ELISPOT-counting, we found that rEg.P29, rEg.P29₈₆₋₁₀₀, and rEg.P29₈₆₋₁₀₅ elicited mononuclear cells isolated from rEg.P29 + FCA-, and rEg.P29 + CpG-immunized mice to produce IFN- γ ([Figure 4A,B](#)), demonstrating a dominant T-cell epitope at this location. In contrast, rEg.P29, rEg.P29₈₆₋₁₀₀, and rEg.P29₈₆₋₁₀₅ were unable to stimulate IL-4 production ([Figure 4C,D](#)).

To determine the cell subsets exhibiting a response to rEg.P29₈₆₋₁₀₀ and rEg.P29₈₆₋₁₀₅, we analyzed lineage differentiation of IFN- γ -producing cells by flow cytometry. T cells producing IFN- γ were CD4⁺ T cells and CD8⁺ T cells; however, the IFN- γ ⁺T cells induced by the overlapping peptides were slightly lower than those induced by rEg.P29 ([Figure 4E,F](#)). Furthermore, as shown in [Figure 4G](#), there was no significant difference in IFN- γ ⁺T cells between rEg.P29₈₆₋₁₀₀ and rEg.P29₈₆₋₁₀₅ groups. Given that epitopes are the smallest units of immune function in antigens, we proposed that a T cell epitope exists within amino acids 86–100 of rEg.P29, and this epitope could induce a dominant T cell response specific to rEg.P29.

rEg.P29₈₆₋₁₀₀ and rEg.P29 activate specific CD4⁺ and CD8⁺ T cells

We detected CD69 and CD25 expressions to evaluate the kinetics of cell activation by flow cytometry. After cells were cultured with 15 μ g/mL of rEg.P29 or rEg.P29₈₆₋₁₀₀, and 1 μ g/mL anti-CD28 antibody, CD4⁺ T cells showed elevated expressions of CD69 and CD25 beginning on day 1 ([Figure 5A–C](#)). The level of CD69 expression in CD4⁺ T cells was decreased on day 3. The level of CD69 expression on CD4⁺ T cells after treatment with rEg.P29 or rEg.P29₈₆₋₁₀₀ was significantly different from the frequencies for cells cultured without rEg.P29 or rEg.P29₈₆₋₁₀₀ on day 1. In addition, after treatment with rEg.P29 or rEg.P29₈₆₋₁₀₀, CD25-expressing cells were significantly elevated on day 3 compared with that in the group without rEg.P29 or rEg.P29₈₆₋₁₀₀, suggesting that most rEg.P29-specific CD4⁺ T cells were already activated on day 3 by rEg.P29 or rEg.P29₈₆₋₁₀₀. It is worth noting that rEg.P29₈₆₋₁₀₀ induced a lower increase in CD69 than rEg.P29; however, there was no significant difference in the magnitude of CD25 elevation between rEg.P29 and rEg.P29₈₆₋₁₀₀.

CD8⁺ T cells were also activated ([Figure 5D–F](#)). The level of CD69 expression on CD8⁺ T cells in rEg.P29- or rEg.P29₈₆₋₁₀₀-activated cells was significantly different from that in cells cultured without rEg.P29 or rEg.P29₈₆₋₁₀₀ on day 1. The level of CD69 expression in CD8⁺ T cells was decreased on day 3. The increase in CD25-expressing cells after culture with rEg.P29 or rEg.P29₈₆₋₁₀₀ was significantly elevated on day 3 compared with that in the control group. Similar to that in CD4⁺ T cells, rEg.P29₈₆₋₁₀₀ induced a lower level of CD69 elevation in CD8⁺ T cells than rEg.P29; however, there was no significant difference in the level of CD25 elevation between rEg.P29 and rEg.P29₈₆₋₁₀₀. The timing of elevations in CD25 and CD69 expressions differed slightly between the rEg.P29 + FCA and rEg.P29 + CpG groups.

rEg.P29₈₆₋₁₀₀ and rEg.P29 promote the proliferation of CD4⁺ and CD8⁺ T cells

Next, we used a CFSE labeling approach to estimate cell proliferation as a parameter for cell expansion. After cultured with rEg.P29 or rEg.P29₈₆₋₁₀₀, the CFSE intensity of a portion of CD4⁺ T cells was

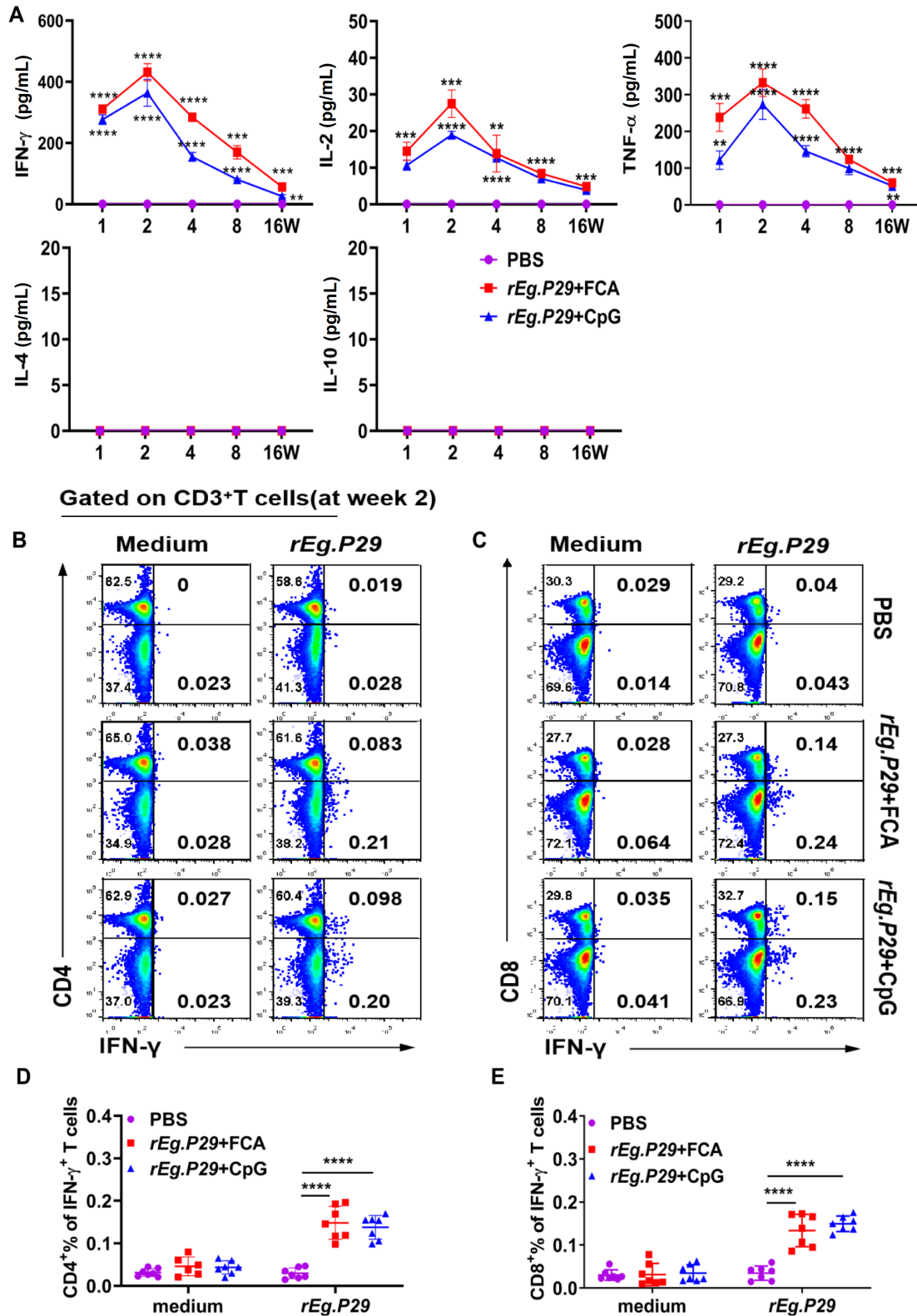


Figure 2. rEg.P29 immunization induced a cellular immune response Mice were primed and boosted with PBS, rEg.P29 + FCA, or rEg.P29 + CpG, following the prime-boost protocol. (A) At the indicated time intervals, mice were sacrificed and mononuclear cells were isolated from the spleen and stimulated with rEg.P29. The supernatants were tested for cytokine production by ELISA. Brefeldin A was added to the culture during the final 6 h. The cells were harvested and stained with fluorochrome-conjugated monoclonal antibodies for lineage differentiation and intracellular cytokine expression assays. Cells were analyzed by flow cytometry and data were analyzed using FlowJo. (B,C) Representative dot plots showing the identification of IFN- γ -producing T cells. (D,E) Frequencies of IFN- γ -producing CD4⁺ T cells and CD8⁺ T cells in the immunization groups are shown. Data were obtained from seven mice. **** $P < 0.0001$, *** $P < 0.001$, ** $P < 0.01$, and ns, $P > 0.05$.

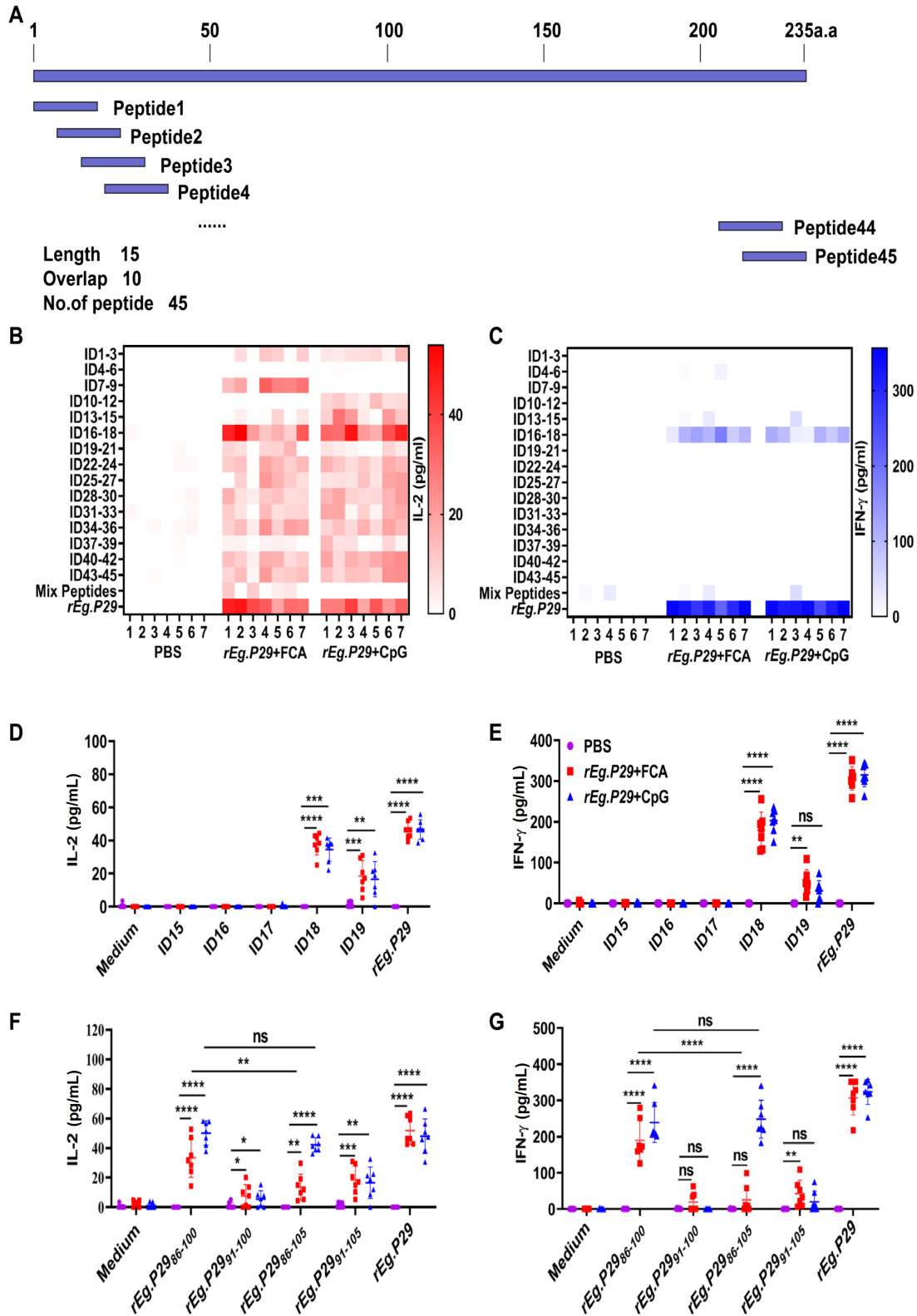


Figure 3. Overlapping peptide screening of T-cell epitopes Mice were primed and boosted with PBS, rEg.P29 + FCA, or rEg.P29 + CpG and sacrificed at week 2 after boosting. Mononuclear cells were isolated from the spleen. (A) Design of individual overlapping peptides. (B,C) Cells were stimulated with a mixture of the peptides and rEg.P29. The medium for dissolving the peptides was used as the control. IFN- γ and IL-2 production in the supernatant were assessed by ELISA. (D,E) Cells were stimulated with rEg.P29, ID15, ID16, ID17, ID18, ID19 and medium, the levels of IFN- γ and IL-2 were detected by ELISA. (F,G) Cells were stimulated with rEg.P29, rEg.P29₈₆₋₁₀₀, rEg.P29₉₁₋₁₀₀, rEg.P29₈₆₋₁₀₅, rEg.P29₉₁₋₁₀₅, or medium, and then the levels of IFN- γ and IL-2 were detected by ELISA. Data were obtained from 7 mice and are expressed as the mean \pm SD. **** P < 0.0001, *** P < 0.001, ** P < 0.01, * P < 0.05, and ns, P > 0.05.

Table 2. Amino acid sequence of the dominant peptides

Peptide name	Sequence	Length
rEg.P29 ₈₆₋₁₀₀	ALEQVASQSEKAAPQ	15
rEg.P29 ₉₁₋₁₀₅	ASQSEKAAPQLSKML	15
rEg.P29 ₉₁₋₁₀₀	ASQSEKAAPQ	10
rEg.P29 ₈₆₋₁₀₅	ALEQVASQSEKAAPQLSKML	20

decreased on day 3 and further decreased on day 5 (Figure 6A,C). rEg.P29 and rEg.P29₈₆₋₁₀₀ also promoted the proliferation of CD8⁺ T cells. When cultured with rEg.P29 or rEg.P29₈₆₋₁₀₀, the CFSE intensity of a portion of CD8⁺ T cells was decreased on day 3 and further decreased on day 5 (Figure 6 B,D). However, the ability of rEg.P29₈₆₋₁₀₀ in promoting CD4⁺ T cell proliferation was weaker than that of rEg.P29, while no difference was found in promoting CD8⁺ T cell proliferation between rEg.P29 and rEg.P29₈₆₋₁₀₀.

rEg.P29₈₆₋₁₀₀ is relatively conserved among different isolates of *E. granulosus*

To explore the conservation of the core epitope, we aligned the amino acid sequences of ten distinct genotypes (G1–G10) of *E. granulosus s.l.* AHA85395 (*E. canadensis*) shares a sequence similarity of 93.3% in the position of the rEg.P29₈₆₋₁₀₀ epitope (ALEQVASQSEKAAPQ), with 1 amino acid difference at the thirteenth residue. Other *E. granulosus s.l.* isolates share 100% sequence similarity with rEg.P29₈₆₋₁₀₀ (Figure 7A).

Localization of rEg.P29₈₆₋₁₀₀ on the P29 protein

A three-dimensional model of the P29 protein was constructed based on templates on the SWISS-MODEL server website (Figure 7B). Two monomer templates, *2d4c.1.A* and *6up6.1*, were selected for construction based on the score that combined the highest sequence coverage and sequence similarity. rEg.P29₈₆₋₁₀₀ (ALEQVASQSEKAAPQ) was predicted on the surface of the P29 protein.

Discussion

The control of *E. granulosus* relies on preventing *E. granulosus s.l.* transmission by interventions in dogs and livestock [23]. Primary prevention measures aiming at avoiding the ingestion of *Echinococcus* eggs may reduce the burden of human CE. Additionally, vaccines play an important role in primary prevention [24].

The Eg95 vaccine is a commercial vaccine against *E. granulosus*. It confers 96%–98% protection in sheep, and previous studies have shown that the vaccine is effective [25–27]. However, the Eg95 vaccine mainly targets the G1 genotype and may not be effective against other genotypes, such as G6. Hence, we attempted to produce a multi-epitope vaccine which is able to provide broad protection against *E. granulosus* genotypes. Previous studies have identified rEg.P29 as a candidate molecule for *E. granulosus* vaccine development [12]. However, whole antigen immunization has some limitations [28]; for example, antigenicity is influenced by the expression system. With advances in reverse vaccinology, multi-epitope vaccines are now used in many applications [29,30]. In addition, epitope vaccines have high specificity, and the design of epitope vaccine is flexible, with the ability to combine different T and B cell antigen epitopes. Therefore, epitope vaccines are an important area of research.

The early epitope vaccines mainly consisted of B cell epitopes, which could only elicit a single humoral immune response. The

humoral immune response requires the activity and regulation of the cellular immune response. Several recent studies have demonstrated that a protective B cell epitope is essential for epitope vaccines [31], and the presence of T cell epitopes in epitope vaccine constructs can significantly improve the level of immunoprotection [32–34]. Our previous research did not reveal the dominant role of humoral or cellular immunity in rEg.P29 protection. Therefore, in this study, we filtered out multi-epitope vaccines composed of a T cell epitope from rEg.P29. To determine which peptide can induce a robust T cell response, we searched for dominant epitopes from an overlapping peptide library to screen the epitope peptides against rEg.P29 of *E. granulosus*.

Using a mouse model, we demonstrated that rEg.P29 immunization elicited a Th1-type response. After prime and boost doses of rEg.P29, the cytokine-producing cells peaked at week 2. Most cytokine-producing cells expressed IFN- γ , IL-2, and TNF- α , and a few expressed IL-4 and IL-10. Cytokine production was maintained for at least 16 weeks. Moreover, rEg.P29 could stimulate the induction of IFN- γ production by CD4⁺ and CD8⁺ T cells. Importantly, we found that rEg.P29 contains a murine T cell-specific epitope within amino acids 86–100 (rEg.P29₈₆₋₁₀₀). The level of IFN- γ and number of IFN- γ -producing cells induced by rEg.P29₈₆₋₁₀₀ and rEg.P29₈₆₋₁₀₅ were slightly lower than those induced by rEg.P29. Results for rEg.P29₈₆₋₁₀₀ (15 aa) and rEg.P29₈₆₋₁₀₅ (20 aa) indicated that both CD4⁺ and CD8⁺ T cells contribute to IFN- γ production. These results may be explained by the fact that rEg.P29₈₆₋₁₀₀ and rEg.P29₈₆₋₁₀₅ contain both CD4⁺ T and CD8⁺ T cell epitopes. We ultimately chose the shortest and most effective epitope, rEg.P29₈₆₋₁₀₀ (15 aa), as the T-cell peptide of rEg.P29. The level and number of IFN- γ -producing cells induced by rEg.P29₈₆₋₁₀₀ were the same as those for rEg.P29₈₅₋₁₀₅ but lower than those induced by rEg.P29. Interestingly, T cell responses were restricted to long peptides and were not induced by stimulation with 10-mer peptides, in line with the results of Schumacher *et al.* [13]. Additionally, rEg.P29- or rEg.P29₈₆₋₁₀₀-induced CD4⁺ and CD8⁺ T cells showed a rapid increase in the expression of CD69 one day after encountering the cognate antigen, with a much higher frequency of CD69 expression than that for cells without induction by rEg.P29 or rEg.P29₈₆₋₁₀₀. CD69 expression was substantially declined and CD25 expression was increased on day 3. These data suggested that rEg.P29- or rEg.P29₈₆₋₁₀₀-specific CD4⁺ and CD8⁺ T cells respond rapidly to *E. granulosus* challenges and establish an efficient adaptive immune response at the early stage of pathogen invasion. However, peptides are limited by weak immunogenicity, and rEg.P29₈₆₋₁₀₀ had a weaker effect on specific T-cell activation than rEg.P29. Both rEg.P29 and rEg.P29₈₆₋₁₀₀ could induce the proliferation of specific CD4⁺ and CD8⁺ T cells.

Ten distinct genotypes (G1–G10) of *E. granulosus s.l.* have already been documented and are named according to their most commonly identified intermediate host [22]. The majority of these genotypes are known to infect humans, with the exception of the G4 horse strain, which has not been reported to be zoonotic in literature. We detected high sequence similarity between rEg.P29₈₆₋₁₀₀ (ALEQVASQSEKAAPQ) and the corresponding positions in AHA85395 (*E. canadensis*), with only one amino acid difference, and 100% similarity between other *E. granulosus s.l.* isolates and rEg.P29₈₆₋₁₀₀. These results are promising for the development of vaccines that are able to protect against a wider range of genotypes. Furthermore, as determined by three-dimensional homology mod-

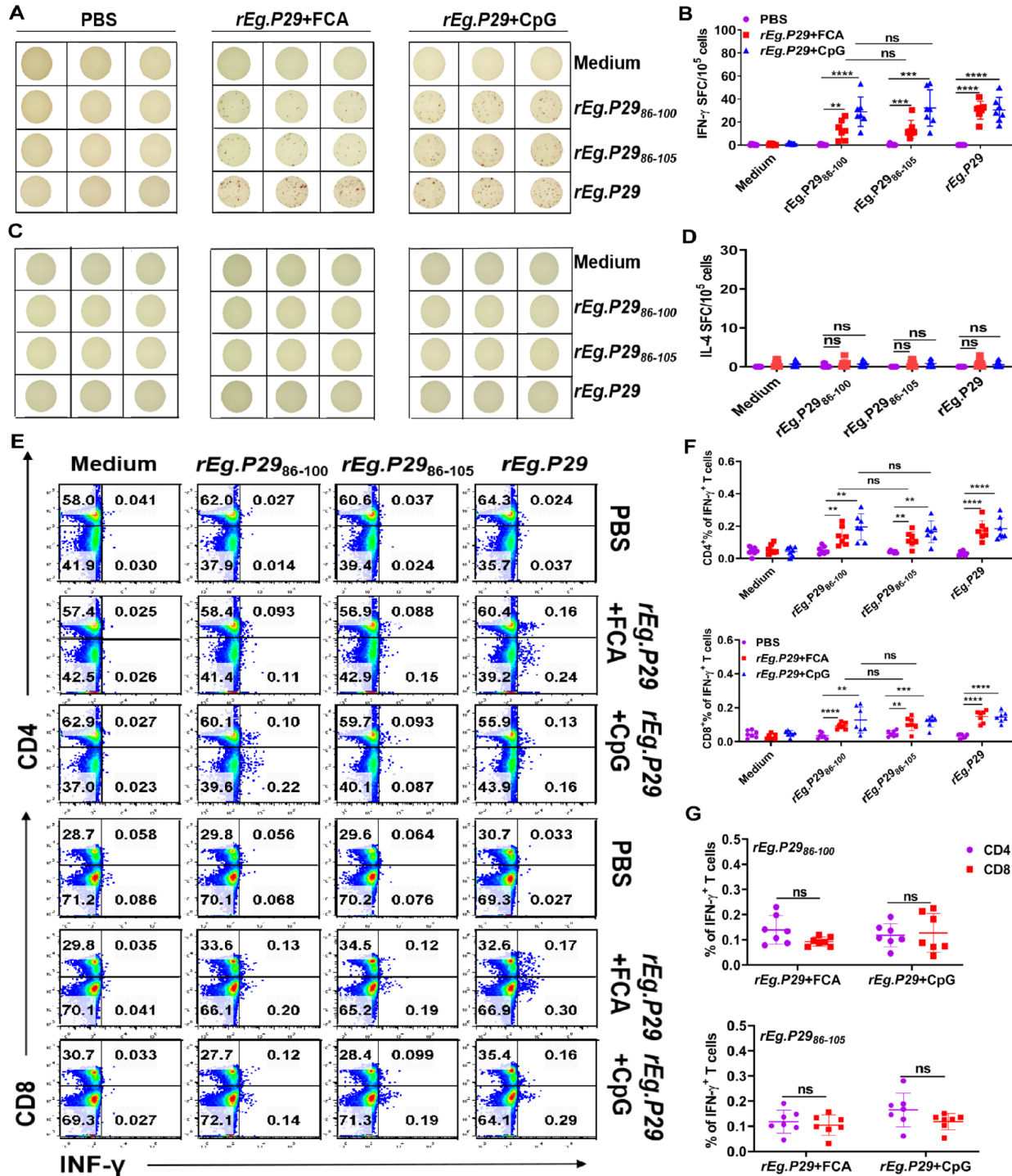


Figure 4. Ability of T-cell epitope peptides to stimulate cytokine production Mice were primed and boosted with PBS, rEg.P29 + FCA, or rEg.P29 + CpG, and sacrificed at week 2 after boosting. Mononuclear cells were isolated from the spleen. (A–D) Cells were stimulated with rEg.P29₈₆₋₁₀₀, rEg.P29₈₆₋₁₀₅, rEg.P29, or medium, and cells producing IFN- γ and IL-4 were counted by ELISPOT. The cells were harvested and stained with fluorochrome-conjugated monoclonal antibodies for lineage differentiation and intracellular cytokine expression assays. Cells were analyzed by flow cytometry and data were analyzed using FlowJo. (E) Representative dot plots showing IFN- γ -producing CD4⁺ T and CD8⁺ T cells in the immunization groups. (F) Frequencies of IFN- γ -producing CD4⁺ T and CD8⁺ T cell populations from the rEg.P29 + FCA and rEg.P29 + CpG groups are shown. Data were obtained from 7 mice and are expressed as the mean \pm SD. **** $P < 0.0001$, *** $P < 0.001$, ** $P < 0.01$, and ns, $P > 0.05$.

eling, rEg.P29₈₆₋₁₀₀ is on the surface of rEg.P29, facilitating binding to antigenic epitopes.

In our prime and boost procedure, adjuvant CpG promoted the

immunogenicity of rEg.P29. The use of CpG was based on other studies, and Freund’s adjuvant was used as a control. In addition, CpG ODN was approved in 2017 by the FDA as an adjuvant for the

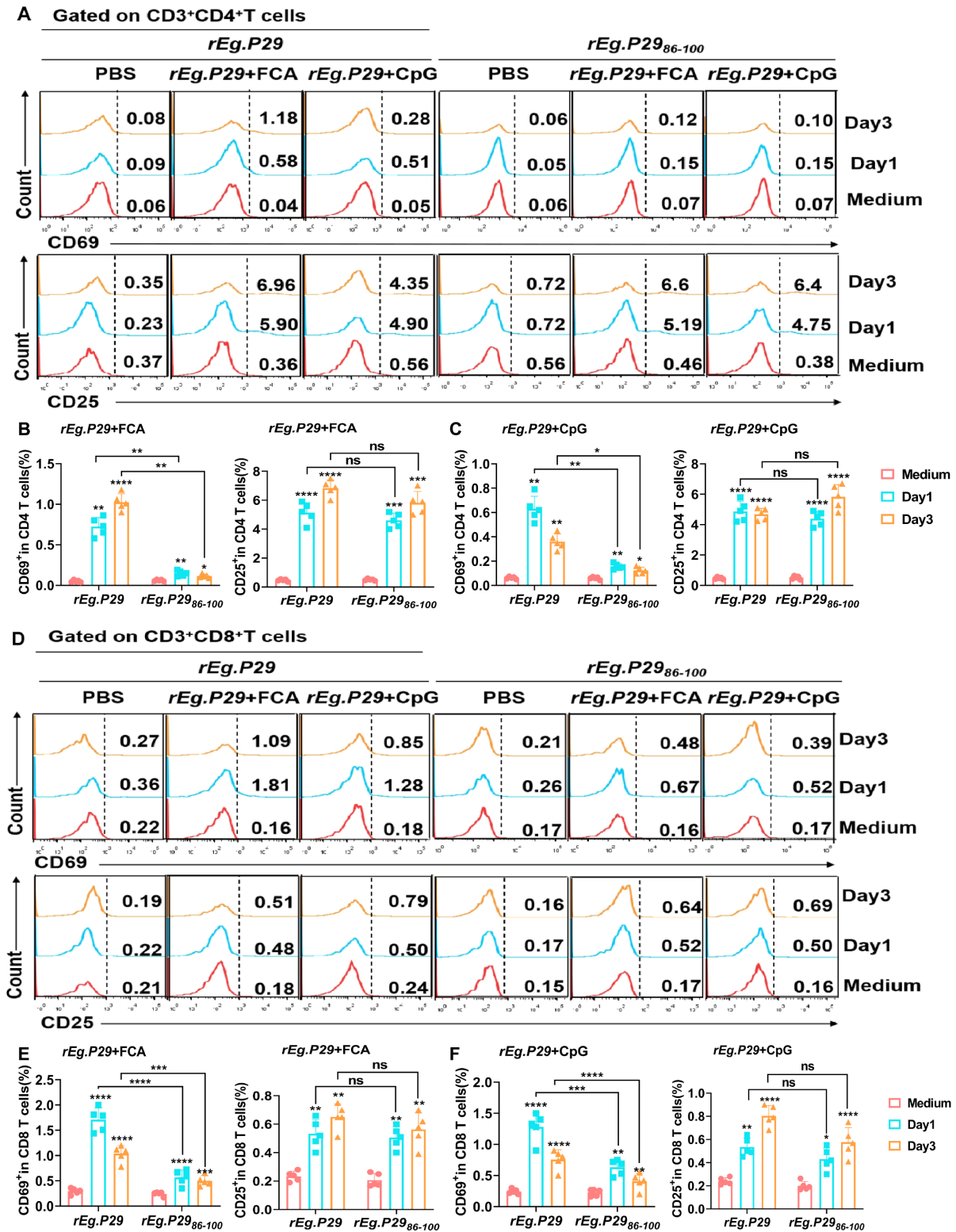


Figure 5. rEg.P29₈₆₋₁₀₀ and rEg.P29 activate specific CD4⁺ and CD8⁺ T cells. Mice were primed and boosted with PBS, rEg.P29 + FCA, or rEg.P29 + CpG, and sacrificed at week 2 after boosting. Mononuclear cells were isolated from the spleen. (A–C) Cells were stimulated with rEg.P29₈₆₋₁₀₀, rEg.P29, or medium for 1 and 3 days. The cells were harvested and stained with fluorochrome-conjugated monoclonal antibodies for CD69 and CD25. Cells were analyzed by flow cytometry and data were analyzed using FlowJo. (A) Representative dot plots showing CD69 and CD25 expressions in CD4⁺ T cells. (B,C) Frequencies of CD69 and CD25 expression in CD4⁺ T cells from rEg.P29 + FCA and rEg.P29 + CpG groups. (D) Representative dot plots showing CD69 and CD25 expressions in CD8⁺ T cells. (E,F) Frequencies of CD69 and CD25 expression in CD8⁺ T cells from rEg.P29 + FCA and rEg.P29 + CpG groups are shown. Data were obtained from 5 mice and are expressed as the mean ± SD. *****P* < 0.0001, ****P* < 0.001, ***P* < 0.01, **P* < 0.05, and ns, *P* > 0.05.

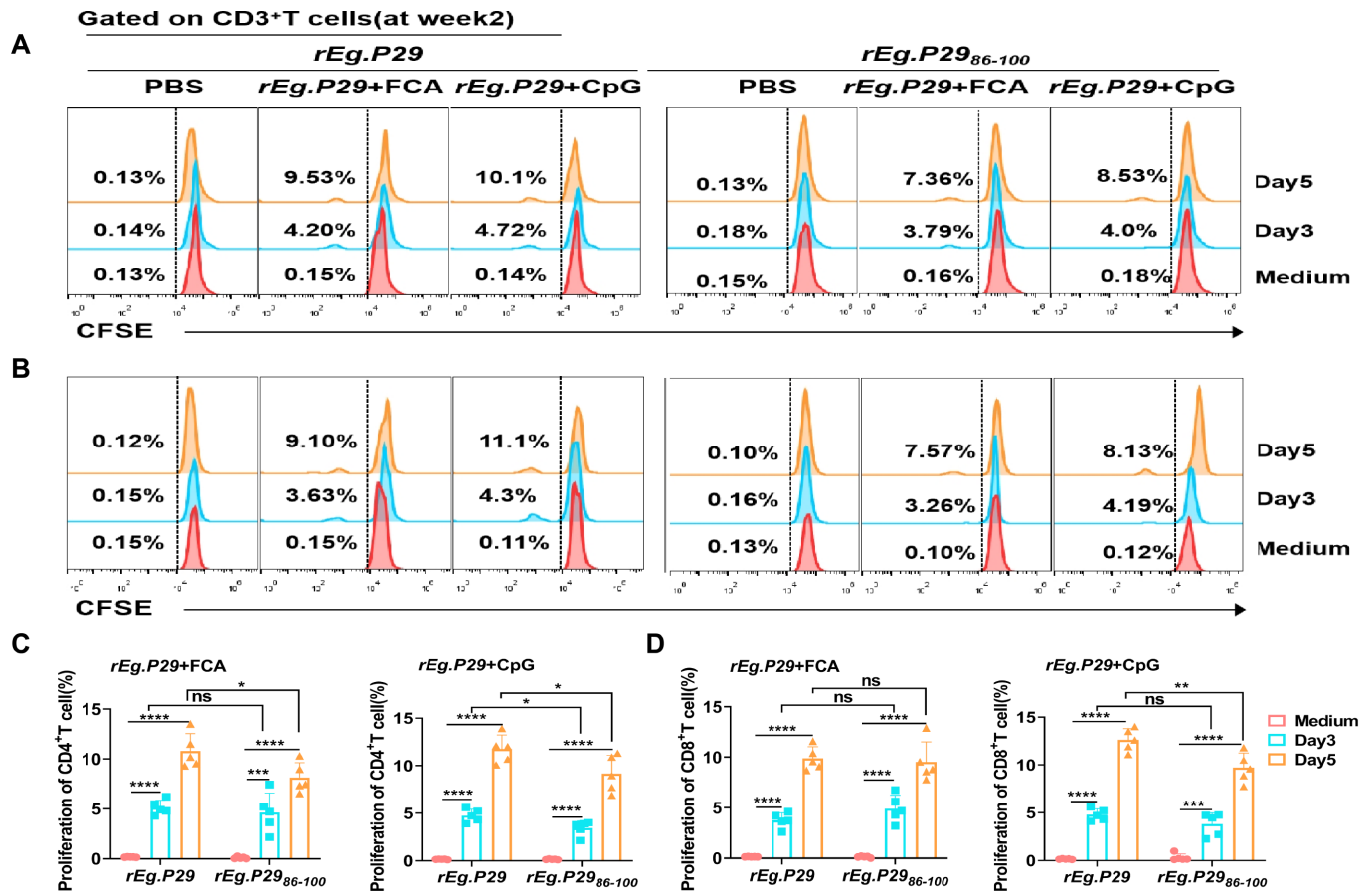


Figure 6. Specific CD4⁺ and CD8⁺ T cell proliferation Mice were primed and boosted with PBS, rEg.P29 + FCA, or rEg.P29 + CpG and sacrificed at week 2 after boosting. Mononuclear cells were isolated from the spleen. Cells were used for CFSE labeling and stimulated with rEg.P29₈₆₋₁₀₀, rEg.P29, or medium for 3 and 5 days. The cells were harvested and stained with fluorochrome-conjugated monoclonal antibodies for CD4 and CD8. Cells were analyzed by flow cytometry and data were analyzed using FlowJo. (A,B) Representative dot plots showing the identification of proliferative CD4⁺ and CD8⁺ T cells. (C,D) Frequencies of proliferative CD4⁺ and CD8⁺ T cells from rEg.P29 + FCA and rEg.P29 + CpG groups. Data were obtained from 5 mice and are expressed as the mean \pm SD. **** $P < 0.0001$, *** $P < 0.001$, ** $P < 0.01$, * $P < 0.05$, and ns, $P > 0.05$.

human hepatitis B virus vaccine HEPLISAV-BTM (Dynavax, Emeryville, USA). Adjuvant CpG enhanced the antigen-specific Th1-type immune response and increased antibody levels. In view of its safety, we chose CpG as the adjuvant. It is important to note that adjuvants (e.g., FCA and CpG) in this study did not independently induce a T cell response without rEg.P29 or rEg.P29₈₆₋₁₀₀, as shown in [Supplementary Figure S2](#). Adjuvants have been shown to significantly enhance the immune effect without inducing a specific immune response [35]. We did not determine the immunoprotective effects of peptide vaccines. However, we screened the T cell epitope of rEg.P29 from the overlap library to provide a reference for the next step in epitope vaccine research.

In conclusion, rEg.P29, as a whole antigen, can induce a cellular immune response and contains a T cell epitope (rEg.P29₈₆₋₁₀₀). This study provides a reference for the development of novel and universal multi-epitope vaccines against *E. granulosus*.

Supplementary Data

Supplementary data is available at *Acta Biochimica et Biophysica Sinica* online.

Funding

This work was supported by the grants from the Key R&D Projects

(Major Science and Technology Projects) (No. 2019BCG01001), the Key Projects of the Natural Science Foundation of Ningxia Hui Autonomous Region (No. 2020AAC02039), the Ningxia Hui Autonomous Region Key Research Program (No. 2018BEG02003), the Natural Science Foundation of Ningxia Hui Autonomous Region (No. NZ15212) and the Natural Science Foundation of Ningxia Hui Autonomous Region (No. 2021AAC03407).

Conflict of Interest

The authors declare that they have no conflict of interest.

References

- Schweiger A, Ammann RW, Candinas D, Clavien PA, Eckert J, Gottstein B, Halkic N, *et al.* Human alveolar echinococcosis after fox population increase. *Emerg Infect Dis* 2007, 13: 878–882
- Working to overcome the global impact of neglected tropical diseases—Summary. *Wkly Epidemiol Rec* 2011, 86: 113–120
- Wen H, Vuitton L, Tuxun T, Li J, Vuitton DA, Zhang W, McManus DP. Echinococcosis: advances in the 21st Century. *Clin Microbiol Rev* 2019, 32:
- Brunetti E, Kern P, Vuitton DA. Expert consensus for the diagnosis and treatment of cystic and alveolar echinococcosis in humans. *Acta Tropica* 2010, 114: 1–16
- Nabarro LE, Amin Z, Chiodini PL. Current management of cystic echi-

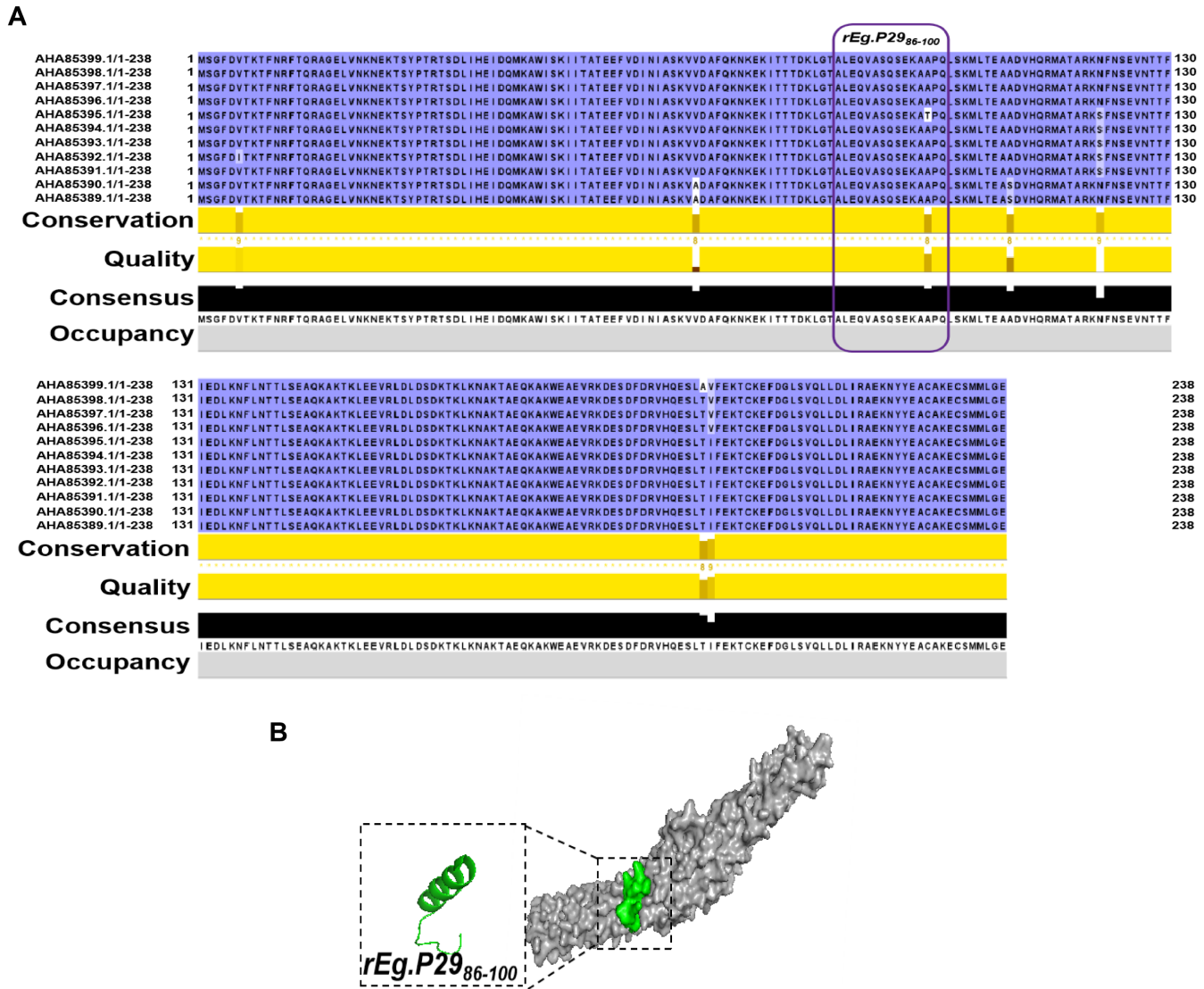


Figure 7. Multiple sequence alignment (A) Amino acid sequence homology was analyzed using BLAST and Jalview. (B) Model of the 3D structure of the P29 protein predicted by SWISS-MODEL. The overall structure is shown, with the peptide structure for T-cells, rEg.P29₈₆₋₁₀₀ (ALEQVASQSEKAAPQ) marked in green.

- nococcosis: a survey of specialist practice. *Clin Infect Dis* 2015, 60: 721–728
- Lissandrin R, Tamarozzi F, Mariconti M, Manciuoli T, Brunetti E, Vola A. Watch and wait approach for inactive echinococcal cyst of the liver: an update. *Am J Tropical Med Hyg* 2018, 99: 375–379
 - Stojković M, Weber TF, Junghans T. Clinical management of cystic echinococcosis. *Curr Opin Infect Dis* 2018, 31: 383–392
 - Gottstein B, Stojkovic M, Vuitton DA, Millon L, Marcinkute A, Deplazes P. Threat of alveolar echinococcosis to public health—a challenge for Europe. *Trends Parasitology* 2015, 31: 407–412
 - Excler JL, Saville M, Berkley S, Kim JH. Vaccine development for emerging infectious diseases. *Nat Med* 2021, 27: 591–600
 - González G, Spinelli P, Lorenzo C, Hellman U, Nieto A, Willis A, Salinas G. Molecular characterization of P-29, a metacestode-specific component of *Echinococcus granulosus* which is immunologically related to, but distinct from, antigen 5. *Mol Biochem Parasitology* 2000, 105: 177–185
 - Liang Y, Song H, Wu M, Xie Y, Gu X, He R, Lai W, *et al.* Preliminary evaluation of recombinant EPC1 and TPx for serological diagnosis of animal cystic *Echinococcosis*. *Front Cell Infect Microbiol* 2020, 10: 177
 - Wang H, Li Z, Gao F, Zhao J, Zhu M, He X, Niu N, *et al.* Immunoprotection of recombinant Eg.P29 against *Echinococcus granulosus* in sheep. *Vet Res Commun* 2016, 40: 73–79
 - Schumacher T, Bunse L, Pusch S, Sahn F, Wiestler B, Quandt J, Menn O, *et al.* A vaccine targeting mutant IDH1 induces antitumour immunity. *Nature* 2014, 512: 324–327
 - Li J, Zhao J, Shen J, Wu C, Liu J. Intranasal immunization with *Mycobacterium tuberculosis* Rv3615c induces sustained adaptive CD4⁺ T-cell and antibody responses in the respiratory tract. *J Cell Mol Med* 2019, 23: 596–609
 - Huang HJ, Curin M, Banerjee S, Chen KW, Garmatiuk T, Resch-Marat Y, Carvalho-Queiroz C, *et al.* A hypoallergenic peptide mix containing T cell epitopes of the clinically relevant house dust mite allergens. *Allergy* 2019, 74: 2461–2478
 - Pourseif MM, Moghaddam G, Naghili B, Saedi N, Parvizpour S, Nema-

- tollahi A, Omidi Y. A novel in silico minigene vaccine based on CD4⁺ T-helper and B-cell epitopes of EG95 isolates for vaccination against cystic echinococcosis. *Comput Biol Chem* 2018, 72: 150–163
17. Biranvand E, Rafiei A, Beiromvand M, Amari A, Bahraini A, Motamedfar A. Cytokine profiles in peripheral blood mononuclear cells from patients with cystic echinococcosis. *Comp Immunol Microbiol Infect Dis* 2020, 70: 101469
 18. Li ZD, Mo XJ, Yan S, Wang D, Xu B, Guo J, Zhang T, *et al.* Multiplex cytokine and antibody profile in cystic echinococcosis patients during a three-year follow-up in reference to the cyst stages. *Parasites Vectors* 2020, 13: 133
 19. Aceti A, Pennica A, Teggi A, Fondacaro LM, Caferro M, Leri O, Tacchi G, *et al.* IgG subclasses in human hydatid disease: prominence of the Igg4 response. *Int Arch Allergy Immunol* 1993, 102: 347–351
 20. García-Luna J, Magnone J, Miles S, López-Santurio C, Dematteis S, Mourglia-Ettlin G. Polyreactive antibodies as potential humoral biomarkers of host resistance to cystic echinococcosis. *Parasite Immunol* 2021, 43: e12802
 21. Wang C, Yang SH, Niu N, Tao J, Du XC, Yang JH, Zhu MX, *et al.* lncRNA028466 regulates Th1/Th2 cytokine expression and associates with *Echinococcus granulosus* antigen P29 immunity. *Parasites Vectors* 2021, 14: 295
 22. Boubaker G, Gottstein B, Hemphill A, Babba H, Spiliotis M. *Echinococcus* P29 antigen: molecular characterization and implication on post-surgery follow-up of CE patients infected with different species of the *Echinococcus granulosus* complex. *PLoS ONE* 2014, 9: e98357
 23. Tamarozzi F, Deplazes P, Casulli A. Reinventing the wheel of *Echinococcus granulosus* sensu lato transmission to humans. *Trends Parasitology* 2020, 36: 427–434
 24. Oscherwitz J. The promise and challenge of epitope-focused vaccines. *Hum Vaccines Immunother* 2016, 12: 2113–2116
 25. Lightowlers MW, Jensen O, Fernandez E, Iriarte JA, Woollard DJ, Gauci CG, Jenkins DJ, *et al.* Vaccination trials in Australia and Argentina confirm the effectiveness of the EG95 hydatid vaccine in sheep. *Int J Parasitology* 1999, 29: 531–534
 26. Prestani M, Dalimi A, Sarvi S, Khoramabadi N. Evaluation of immunogenicity of novel isoform of EG95 (EG95-5G1) from *Echinococcus granulosus* in BALB/C Mice. *Iran J Parasitol* 2014, 9: 491–502
 27. Chow C, Gauci CG, Vural G, Jenkins DJ, Heath DD, Rosenzvit MC, Harandi MF, *et al.* *Echinococcus granulosus*: variability of the host-protective EG95 vaccine antigen in G6 and G7 genotypic variants. *Exp Parasitology* 2008, 119: 499–505
 28. Liu W, Tang H, Li L, Wang X, Yu Z, Li J. Peptide-based therapeutic cancer vaccine: current trends in clinical application. *Cell Prolif* 2021, 54:
 29. Gu Y, Sun X, Li B, Huang J, Zhan B, Zhu X. Vaccination with a paramyosin-based multi-epitope vaccine elicits significant protective immunity against *Trichinella spiralis* infection in mice. *Front Microbiol* 2017, 8: 1475
 30. Pan X, Ke H, Niu X, Li S, Lv J, Pan L. Protection against *Helicobacter pylori* infection in BALB/c mouse model by oral administration of multivalent epitope-based vaccine of cholera toxin B subunit-HUUC. *Front Immunol* 2018, 9: 1003
 31. Ding X, Li H, Li Y, Huang D, Xiong C. Two B-cell epitope vaccines based on uPA effectively inhibit fertility in male mice. *Vaccine* 2018, 36: 2612–2618
 32. Ma J, Wang L, Fan Z, Liu S, Wang X, Wang R, Chen J, *et al.* Immunogenicity of multi-epitope vaccines composed of epitopes from *Streptococcus dysgalactiae* GapC. *Res Vet Sci* 2021, 136: 422–429
 33. Xie W, Zhao W, Zou Z, Kong L, Yang L. Oral multivalent epitope vaccine, based on UreB, HpaA, CAT, and LTb, for prevention and treatment of *Helicobacter pylori* infection in C57BL / 6 mice. *Helicobacter* 2021, 26:
 34. Akhtar N, Joshi A, Kaushik V, Kumar M, Mannan MAU. In-silico design of a multivalent epitope-based vaccine against *Candida auris*. *Microb Pathog* 2021, 155: 104879
 35. Wörzner K, Sheward DJ, Schmidt ST, Hanke L, Zimmermann J, McInerney G, Karlsson Hedestam GB, *et al.* Adjuvanted SARS-CoV-2 spike protein elicits neutralizing antibodies and CD4 T cell responses after a single immunization in mice. *EBioMedicine* 2021, 63: 103197